GROUND'2006 and **2nd LPE**

International Conference on Grounding and Earthing
&
2nd International Conference on Lightning Physics and Effects
Maceió - Brazil November, 2006

SOFTWARE BASED ON MOM MODEL TO ANALYZE ELECTROMAGNETIC TRANSIENTS IN GROUNDING SYSTEMS

Karlo Queiroz da Costa Victor Dmitriev
Federal University of Para - Brazil

Abstract - We present in this work a software based on electromagnetic field theory to analyze transients in grounding systems. In our model, we use the Method of Moments (MoM) to solve numerically the integral equation for the electromagnetic potentials. The equation describes a grounding system constituted by rods. The modified image theory is used to consider the interface air-earth. The MoM software was written in Matlab to analyze systems constituted by vertical and horizontal rods. The numerical results obtained by this software are presented and compared with experimental and theoretical data available in the literature.

1 - INTRODUCTION

The principal objetive of a grounding system is to protect an electric system against short-circuit, accumulation of charges, and lightning discharge [1]. A good grounding system easily guides the excess of charges to the ground. To know the performance of a given grounding system for the case when a lightning discharge occurs, it is necessary to do experiments or numerical simulations by mathematical models.

Theoretical analysis of grounding systems can be classified in two types: low and high frequencies. In low frequencies, one simple equivalent resistence can be used as mathematical model. Examples of equivalent resistence are found in [1]. In high frequencies, there are equivalent impedances for simple grounding systems [2]. Models more elaborated for analysis of transients in such systems are: equivalent circuits [3,4] and transmission lines [5,6].

More accurate theoretical models are those known in the literature as electromagnetic models, since these use the Maxwell's equations. Full wave models in frequency domain (Method of Moments - MoM) is presented in [7,8,9] and in time domain (Finite Difference in Time Domain - FDTD) in [10,11].

In this work we present a software with graphical user interface based on electromagnetic field theory to analyze transients in simple grounding systems composed by horizontal and vertical rods. In the mathematical model we use the MoM [8] to solve the integral equation of the electromagnetic potentials of these grounding systems. In this model, we use sinusoidal basis and test functions. To consider the interface air-earth, we apply the modified image theory [8,12]. The software was developed in Matlab [13].

2 – MATHEMATICAL MODEL

Analysis of transients in grounding systems consists in the evaluation of the voltage on the conductors and near of them when a given transitory current is incident in somewhere of the system. This injected current can represent for example a lightning discharge. In the MoM analysis presented in this section, this current given in the time domain $i(t)$ is transformed to the frequency domain by Discret Transform of Fourier (FFT) and the results in the frequency domain are put in time domain by Inverse Discret Transform of Fourier (IFFT). In Matlab these functions are fft and ifft respectively.

2.1 – INTEGRAL EQUATION FOR POTENTIALS

For a given linear conductor in a uniform medium, it is considered that there is an incident external electric field on the conductor $\bar{E}^i$. This field will induce electrical current in the conductor, and consequently, the induced current will radiate an electric field $\bar{E}^e$ (scattered field). In the case of a lossless conductor, we have the following boundary condition at the surface of the conductor: $\bar{n}\times\bar{E}^e = -\bar{n}\times\bar{E}^i$, $\bar{n}$ is a unit vector normal to the conductor's surface. Starting from the Maxwell's equations, the folowing equations can be obtained to calculate the scattered field:

$$\bar{E}^e(\bar{r}) = -j\omega\bar{A}(\bar{r}) - \nabla\Phi(\bar{r}) \tag{1}$$

$$\bar{A}(\bar{r}) = \mu\int_l \bar{I}(l')g(R)dl' \tag{2}$$

$$\Phi(\bar{r}) = \frac{1}{\varepsilon}\int_l \chi(l')g(R)dl' \tag{3}$$

$$\chi(l') = -\frac{1}{j\omega}\frac{d|\bar{I}(l')|}{dl'} \tag{4}$$

$$g(R) = \frac{e^{-\gamma R}}{4\pi R},\ R = |\bar{r} - \bar{r}'| \tag{5}$$

where $\bar{I}$ is the linear current on the conductor, l the curve that describes the conductor's geometry, $\bar{r}'$ the source point on the curve l, $\bar{r}$ the observation point, l' the curve l in function of $\bar{r}'$, and

$$\gamma^2 = -\omega^2\mu\varepsilon \tag{6}$$

$$\varepsilon = \varepsilon_r\varepsilon_0 + \frac{\sigma}{j\omega} \tag{7}$$

Parameter μ is the permeability; ε_r and ε_0 are the relative permittivity and permittivity of free space respectively, σ the electric conductivity, and ω the angular frequency. The factor $e^{j\omega t}$ is the time variation of the functions in (1)-(5).

The substitution of (2)-(5) in (1) we have the integral equation of potentials for a wire in a uniform medium with a linear current $\bar{I}$. This equation is integral because the current function that we want to obtain is in the integrand.

2.2 – NUMERICAL SOLUTION BY MOM

To solve numerically the integral equation described above by MoM, the first step is to divide the linear conductor in several segments of discretization.

Figure 1 shows a linear conductor of lenght L divided in N straight segments. Two generical segments n e m are shown and their representative vectors are $\overline{\Delta l_n}$ and $\overline{\Delta l_m}$ respectively. The unit tangential vector of each segment is $\overline{a_n}$, thus, $\overline{\Delta l_n} = \Delta l_n \overline{a_n}$.

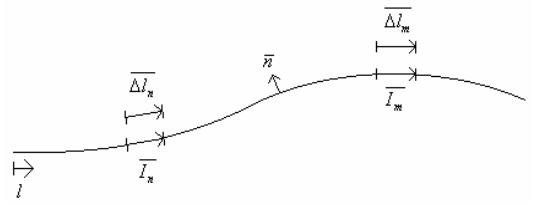

Figure 1 – Two segments of a linear conductor with lenght L

The series expansion of the current used in this work is

$$\bar{I} = \sum_{n=1}^{N} \frac{1}{\sinh\gamma\Delta l_n}\left[I_{n1}\sinh\gamma(l_{n2}-l) + I_{n2}\sinh\gamma(l-l_{n1})\right]\overline{a_n} \qquad (8)$$
$$= \sum_{n=1}^{N} I_n \overline{a_n} = \sum_{n=1}^{N} \overline{I_n}$$

where I_{n1} and I_{n2} are the expansion's coeficients and $I_{12}=I_{21}=I_1,...,I_{n2}=I_{(n+1)1}=I_n,...,I_{(N-1)2}=I_{N1}=I_N$. The expansion (8) in one segment is the sum of two functions sine hiperbolic (sinh) as shown in Figure 2. Figure 3 presents an example of four basis functions existing in a conductor with five segments. Note that in this example the current at the extremities are null ($I_{11}=I_{N2}=0$), but in the case where there is injected current at one extremity, the constant I_{11} or I_{N2} are not null.

Procedure to calculate the coeficients I_n is given as follows. The test functions firstly used in this work are the pulses

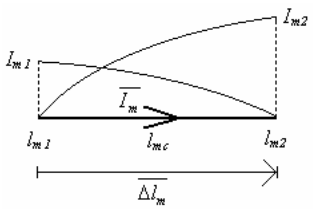

Figure 2 – Sinusoidal expansion in one segment

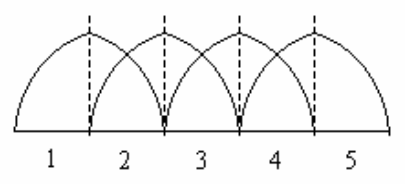

Figure 3 – Example of sinusoidal expansion in a conductor with five segments

$$P_m(l) = \begin{cases} 1 & , \quad l_{mc} < l < l_{(m+1)c} \\ 0 & , \quad \text{elsewhere} \end{cases} \quad m=1,...,N\text{-}1 \qquad (9)$$

l_{mc} is the midle point betwen the points l_{m1} and l_{m2} (Figure 2). Integrating the product of the tangential componente of $\overline{E}^e$ on the wire with one generic test function $P_m(l)$ we have

$$\int_{l_{mc}}^{l_{(m+1)c}} [\overline{E}^e P_m(l)]\cdot\overline{dl} = \int_{l_{mc}}^{l_{(m+1)c}} P_m(l)\left[-j\omega\overline{A} - \nabla\Phi\right]\cdot\overline{dl} \qquad (10)$$

$$\int_{l_{mc}}^{l_{(m+1)c}} E^i dl = \int_{l_{mc}}^{l_{(m+1)c}} \left[j\omega\overline{A} + \nabla\Phi\right]\cdot\overline{a_l} dl \qquad (11)$$

$$\int_{l_{mc}}^{l_{(m+1)c}} E^i dl = \sum_{n=1}^{N}\left\{-\int_{l_{mc}}^{l_{(m+1)c}} L\overline{I_n}\cdot\overline{a_l} dl\right\} \qquad (12)$$

$$L\overline{I_n} = \frac{1}{j\omega\varepsilon}\left(-\gamma^2\int_{l_{n1}}^{l_{n2}}\overline{I_n}(l')g(R)dl' + \int_{l_{n1}}^{l_{n2}}\frac{dI_n}{dl'}\nabla g(R)dl'\right) \qquad (13)$$

E^i is the tangential component of $\overline{E}^i$ on the wire.

If we write the current in the folowing form:

$$\overline{I_n} = I_{n1}\bar{f}_{n1} + I_{n2}\bar{f}_{n2} \qquad (14)$$
$$\bar{f}_{n1} = \frac{\sinh\gamma(l_{n2}-l)}{\sinh\gamma\Delta l_n}\overline{a_n}$$
$$\bar{f}_{n2} = \frac{\sinh\gamma(l-l_{n1})}{\sinh\gamma\Delta l_n}\overline{a_n}$$

we have

$$\int_{l_{mc}}^{l_{(m+1)c}} E^i dl = \sum_{n=1}^{N}\left\{-\int_{l_{mc}}^{l_{(m+1)c}}\left[I_{n1}L\bar{f}_{n1} + I_{n2}L\bar{f}_{n2}\right]\cdot\overline{a_l} dl\right\} \qquad (15)$$

$$\int_{l_{mc}}^{l_{(m+1)c}} E^i dl = -\int_{l_{mc}}^{l_{(m+1)c}} I_{11}L\bar{f}_{11}\cdot\overline{a_l} dl + \sum_{n=1}^{N-1}\left\{-\int_{l_{mc}}^{l_{(m+1)c}}\left[L\bar{f}_{n2} + L\bar{f}_{(n+1)1}\right]\cdot\overline{a_l} dl\right\} I_n - \qquad (16)$$
$$- \int_{l_{mc}}^{l_{(m+1)c}} I_{N2}L\bar{f}_{N2}\cdot\overline{a_l} dl$$

For problems of antennas and scattering we have $I_{11}=I_{N2}=0$, and we obtain the linear system

$$V_m = \sum_{n=1}^{N-1} Z_{mn} I_n \qquad m=1,2,...,N\text{-}1, \qquad (17)$$

$$V_m = \int_{l_{mc}}^{l_{(m+1)c}} E^i dl \tag{18}$$

$$Z_{mn} = -\int_{l_{mc}}^{l_{(m+1)c}} \left[L\bar{f}_{n2} + L\bar{f}_{(n+1)1} \right] \cdot \overline{a}_l dl \tag{19}$$

The values of V_m are related to the excitation source. The solution of (18) gives the coefficients of (8). Similar procedure to that from (10) to (19) can be done with sinusoidal test functions:

$$F_m(l) = \begin{cases} \dfrac{\sinh \gamma (l - l_{m1})}{\sinh \gamma \Delta l_m} & , \; l_{m1} < l < l_{m2} \\ \dfrac{\sinh \gamma (l_{(m+1)2} - l)}{\sinh \gamma \Delta l_{(m+1)}} & , \; l_{m2} < l < l_{(m+1)2} \end{cases} \tag{20}$$

2.3 – ELECTRIC FIELDS RADIATED BY SINUSOIDAL CURRENT ELEMENT

The exact expressions for the electric fields radiated by one sinusoidal current element (Figure 2) are [8]:

$$E_z = \frac{\eta}{4\pi \sinh \gamma d} \left[(I_1 - I_2 \cosh \gamma d) \frac{e^{-\gamma R_2}}{R_2} + (I_2 - I_1 \cosh \gamma d) \frac{e^{-\gamma R_1}}{R_1} \right] \tag{21}$$

$$E_\rho = \frac{\eta}{4\pi\rho \sinh \gamma d} \left\{ (I_1 e^{-\gamma R_1} - I_2 e^{-\gamma R_2}) \sinh \gamma d + \right. \tag{22}$$
$$\left. + (I_1 \cosh \gamma d - I_2) \cos\theta_1 e^{-\gamma R_1} + (I_2 \cosh \gamma d - I_1) \cos\theta_2 e^{-\gamma R_2} \right\}$$

The geometric parameters of these equations are shown in Figure 4.

2.4 – MODIFIED IMAGE THEORY

Supposed we want to calculate the electromagnetic fields

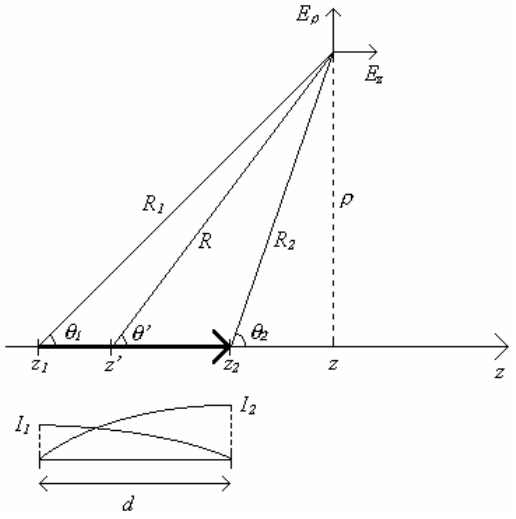

Figure 4 – Local coordenate system used in (21) and (22)

below the ground surface due the current element I shown in Figure 5(a). Using the modified image theory [12] the equvalent problem is that of Figure 5(b), where the medium is uniform with permittivity ε. If we want to calculate the electromagnetic fields above the ground surface due the current element I shown in Figura 5(a) by the the modified image theory, we have equvalent problem shown in Figure 5(c). The ficticious current I' and I'' given in Figure 5 are evaluated by

$$I' = \frac{\varepsilon - \varepsilon_0}{\varepsilon + \varepsilon_0} I \tag{23}$$

$$I'' = \frac{2\varepsilon_0}{\varepsilon + \varepsilon_0} I \tag{24}$$

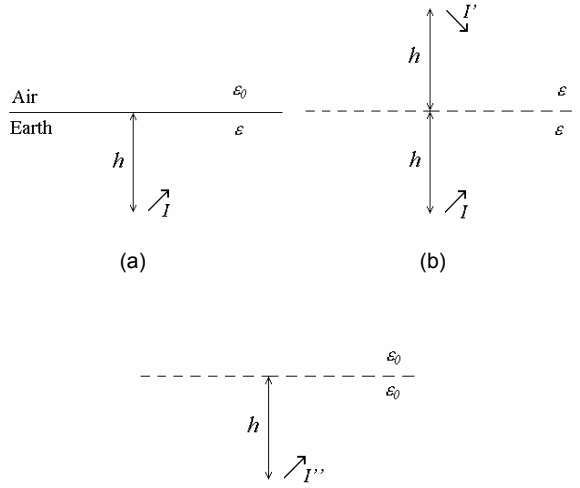

Figure 5 – Application of the modified image theory for grounding systems. (a) real problem. Equivalent problem to compute the electromagnetic fields in the earth (b) and air (c)

3 – TEST OF THE MODEL

To verify the MoM model described above, we present in this section an example of simulation of a MoM code writen in Matlab and compare our results with the theoretical and experimental ones presented in [8]. In this example, we analyze the grounding system shown in Figure 6 composed by one horizontal rod of length L, depth h and radius a. The geometrical parameters of this system are given in Table 1. The source current $i(t)$ is injected in the extremity of the rod (Figure 6). This current is shown in Figure 7.

Table 1 – Parameters used in the simulations

Parameter	Value
L (length)	15 m
h (depth)	0.6 m
a (radius)	12 mm
σ (conductivity of the ground)	(1/70) $(\Omega m)^{-1}$
μ_r	1
ε_r	15

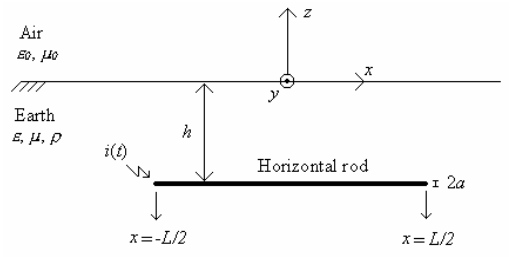

Figure 6 – Grounding system constituted by a horizontal rod

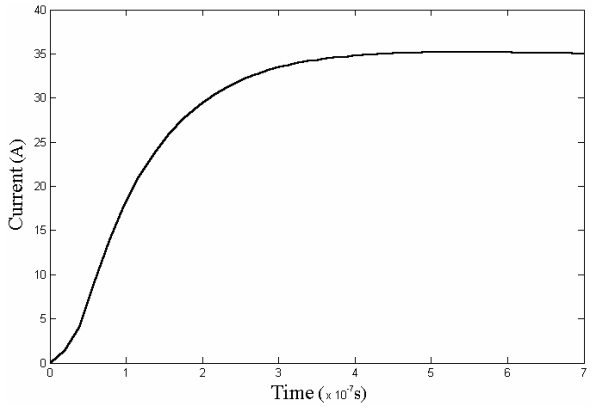

Figure 7 - Current injected in the horizontal rod

Figure 8 present the results calculated here and by the authors of [8] for the potential in different points of the rod. We observe a good agreement of the results in Figure 8. The number of segments of discretization used in this simulation is N=10. We also simulate the same system with N=40, the observed difference between them is about 5-10%.

3 – THE MOM SOFTWARE DEVELOPED

Based on MoM theory presented in previus sections, we developed a graphical user interface in Matlab to analyze two simple grounding systems composed by one vertical rod and one horizontal rod.

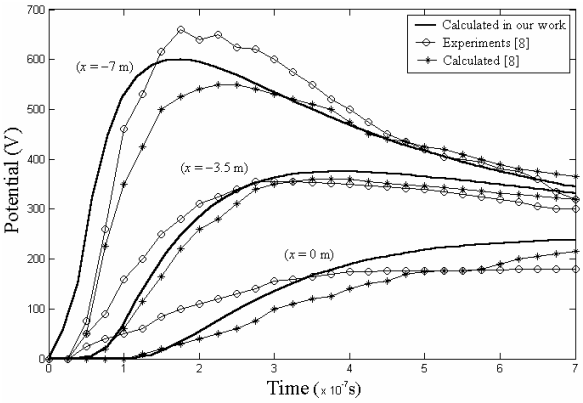

Figure 8 - Potential in different points of the rod

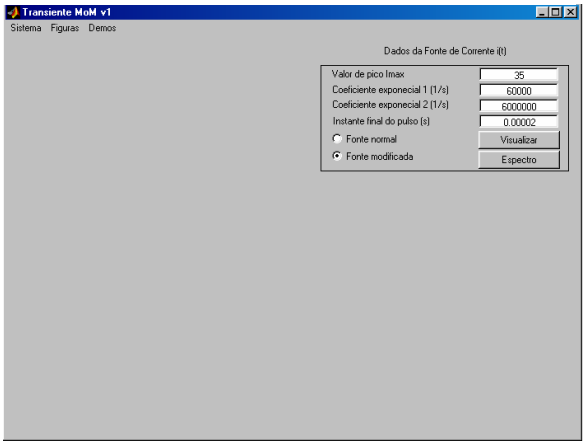

Figure 9 – Main window of the software Transiente MoM v1

The main window of the software Transiente MoM v1 is shown in Figure 9. In the toolbar of this window we have three options: *sistema*, *figuras*, and *demos*. In *sistema* there are two options of systems to analyze (horizontal or vertical rod). The option *figuras* shows the figures of the systems with the notations of the geometrical parameters. In *demos* we have numerical examples of simulations already calculated.

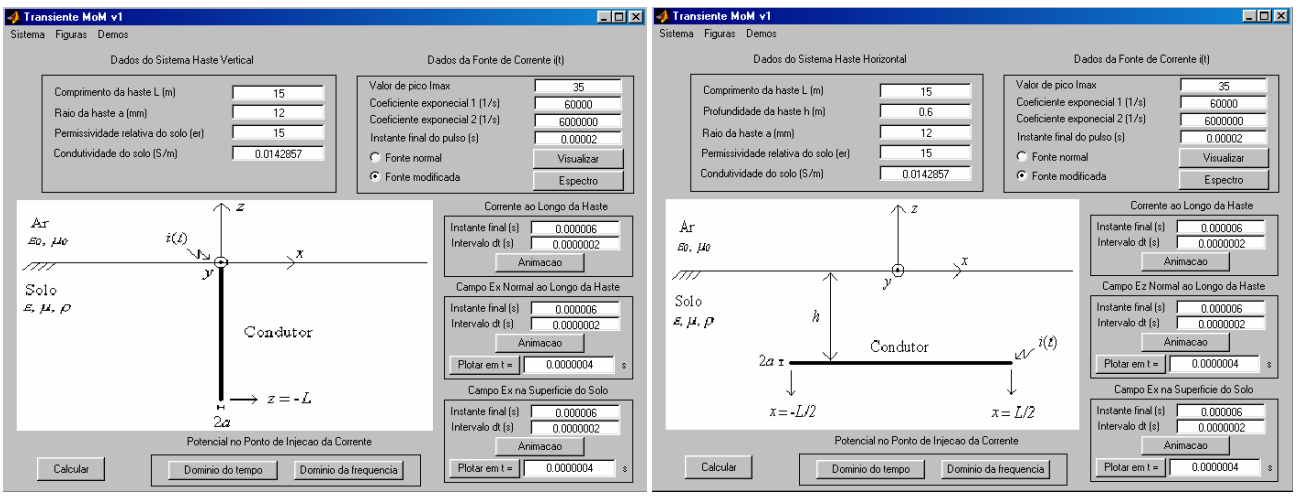

(a) (b)

Figure 10 - Graphical user interface of the software Transiente MoM v1 for simulation of simple grounding systems. (a) vertical rod. (b) horizontal rod

3.1 – NUMERICAL RESULTS

If we choose *sistema* and *horizontal* or *vertical,* one of the windows of the Figure 10 is open. In these windows, we define the parameters of the corresponding system and the injected current that we want to simulate. Two simulations previously calculated are presented in *demos*. The windows of *demos* are the same which are presented in Figure 10. The parameters of the simulations in *demos* are those shown in Figure 10. In the next sections we present some numerical results of the simulations in *demos*.

3.1.1 – POTENTIAL RESPONSE

Injected current used in both systems of the *demos* is the same. The parameters of this current are presented in Figure 10 and the curve in Figure 11. The potential response in time domain obtained for the horizontal and vertical systems are shown in Figure 12 and 13 respectively. We observe a little difference between these results because the injected current, length of the rod, and radius of both systems are the same.

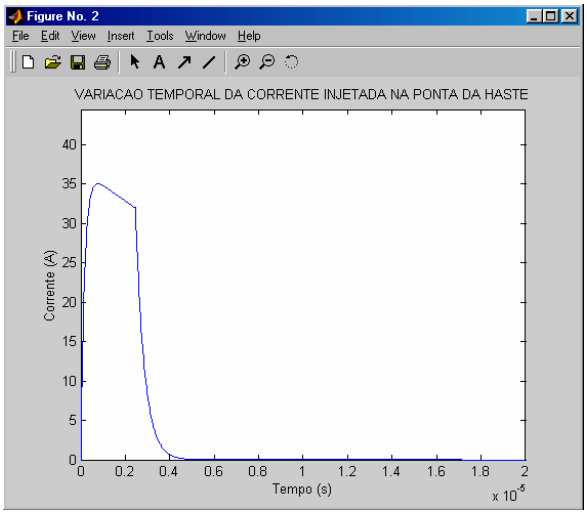

Figure 11 – Injected current in both systems of *demos*

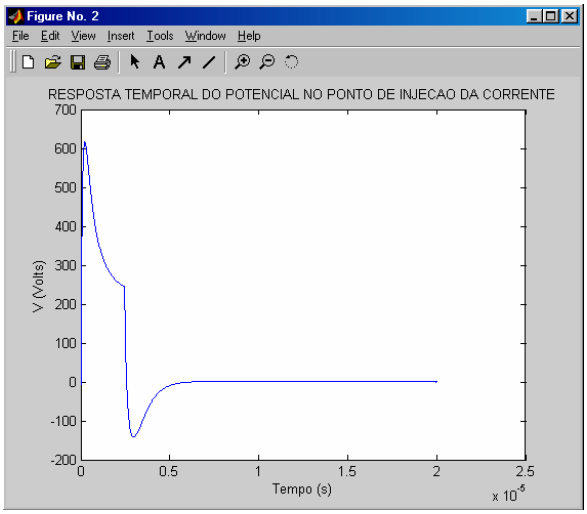

Figure 12 – Potential at the point of current injection of the horizontal system

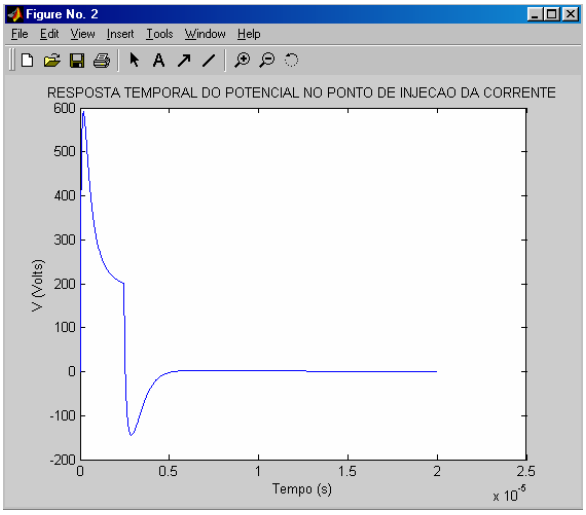

Figure 13 – Potential at the point of current injection of the vertical system

3.1.2 – NORMAL ELECTRIC FIELD ALONG THE ROD

The distribution of the normal electric field along the rod obtained at t=0.4μs for the horizontal and vertical systems are presented in Figure 14 and 15, respectively. We observe in both results the maximum value of the electric field at the extremity where the current is injected, and minimum at other extremity.

3.1.3 – ELECTRIC FIELD ON THE GROUND SURFACE

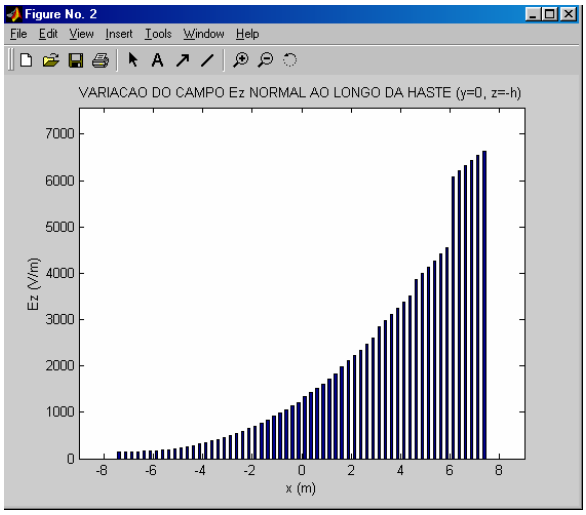

Figure 14 – Distribution of the normal electric field along the horizontal rod at t=0.4μs

The distribution of the tangential electric (E_x) field along the ground surface at t=0.4μs for the horizontal and vertical systems are presented in Figure 16 and 17, respectively. We observe the symmetric distribution of E_x in Figure 17 for the vertical system and maximum value at the point of current injection. For the horizontal system, the distribution of E_x is nonsymmetrical due to the geometry and position of the injected current. For this case, we observe maximum values of E_x near the extremity of the injected current.

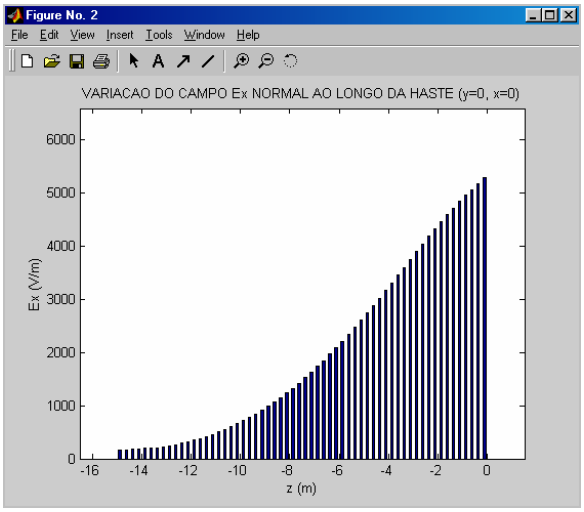

Figure 15 – Distribution of the normal electric field along the vertical rod at t=0.4μs

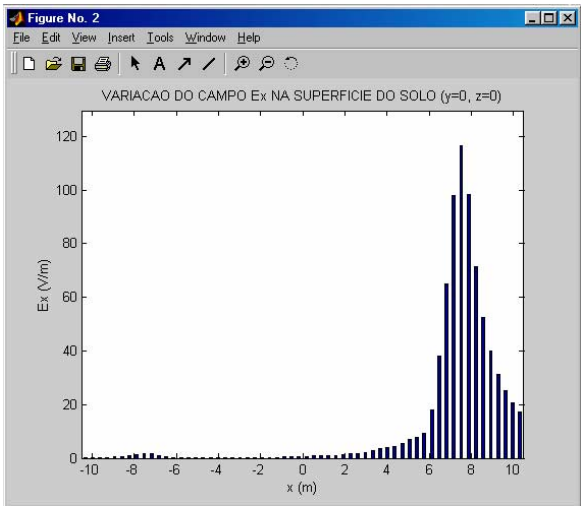

Figure 16 – Distribution of the electric field tangential to the ground surface for the horizontal rod at t=0.4μs

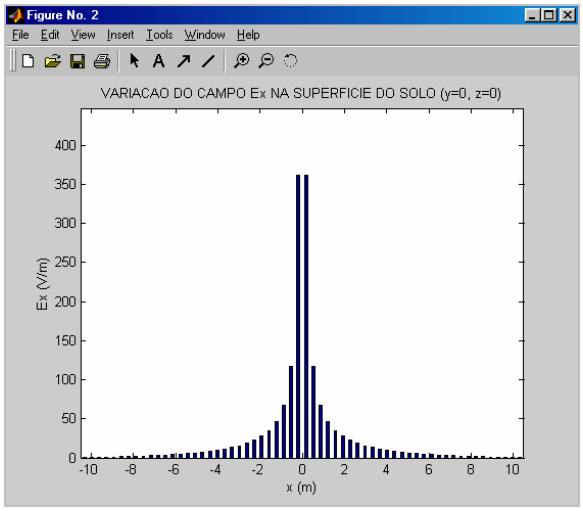

Figure 17 – Distribution of the electric field tangential to the ground surface for the vertical rod at t=0.4μs

4 - CONCLUSIONS

This paper presents a software based on MoM to analyze grounding systems composed of horizontal and vertical rods. In our model, we used sinusoidal basis and test functions, and the modified image theory to consider the interface air-earth. The results presented in this work show a good agreement with theoretical and experimental data obtained by others authors. Thus, our MoM software can be used efficiently to analyze and synthesize conventional grounding systems constituted by vertical and horizontal rods. The software can be modified easily to investigate more complex grounding systems, for example grids.

5 - REFERENCES

[1] G. Kindermann e J. M. Camoagnolo, Aterramento Elétrico, 5a ed., Ed. Florianópolis: UFSC, 2002.
[2] Gono, L. F., Topalis, F. V., Stathopulos, L. A., “Transient impedance of grounding rods,” High Voltage Engineering Symposium, Conference Publication No. 467 – IEE, 22-27 August 1999.
[3] Geri, A., “Behavior of grounding systems excited by high impulse currents: the model and its validation,” IEEE Trans. on Power Delivery, vol. 14, No. 3, pp. 1008-1017, July 1999.
[4] Geri, A., "Sensitivity Analysis of Grounding Systems under Surge Conditions", GROUND'2002 Proceedings, pp. 179-183, Rio de Janeiro – RJ, Brazil, November 2002.
[5] Liu, Y., Zitnik, M., Thottappillil, R., “An improved transmission-line model of grounding system,” IEEE Trans. on Electromagnetic Compatibility, vol. 43, No. 3, pp. 348-355, August 2001.
[6] Almeida, M. E., Correia de Barros, M. T., ""Critical Length” of long Horizontal Ground Electrodes", GROUND'2002 Proceedings, pp. 175-178, Rio de Janeiro – RJ, Brazil, November 2002.
[7] Ala, G., Di Silvestre, M. L., Francomano, E., Tortorici, A., “Wavelet-Based Efficient Simulation of Electromagnetic Transient in a Lightning Protection System,” IEEE Trans. on Magnetics, vol. 39, No. 3, pp. 1257-1260, May 2003.
[8] Grcev, L. D., “Transient electromagnetic fields near large earthing systems,” IEEE Trans. on Magnetics, vol. 32, No. 3, pp. 1525-1528, May 1996.
[9] Grcevski, N., Grcev, L., ”Graphical User Interface for 3D Modeling of Grounding Systems", GROUND'2002 Proceedings, pp. 185-188, Rio de Janeiro – RJ, Brazil, November 2002.
[10] Barberini, S. J., Artuzi Jr., W. A., ”Análise do Campo Elétrico na Interface Ar-Solo em Malhas de Aterramento Usando o Método FDTD", MOMAG'2006, Belo Horizonte – BH, Agosto 2006.
[11] Araújo, H. X., Oliveira, R. M. S., Salame, Y. C., Sobrinho, C. L. S. S., ”Propostas de Novas Técnicas para Redução do Potencial de Passo", MOMAG'2006, Belo Horizonte – BH, Agosto 2006.
[12] Takashima, T., Nakae, T., Ishibashi, R., “High fraquency characteristics of impedances to ground and field distributions of ground electrodes,” IEEE Trans. on Power Apparatus and Systems, vol. PAS-100, No. 4, pp. 1893-1900, April 1981.
[13] Hanselman, D., Littlefeield, B., MATLAB 6: Curso Completo, Ed. São Paulo: Prentice Hall, 2003.

Main author
Name: Karlo Queiroz da Costa
Address: Departamento de Engenharia Elétrica e Computação, Universidade Federal do Pará, Av. Augusto Corrêa no 1, CEP 66075-900, CP 8619, Belém-Pa, Brasil
Fax: +55-12-91-31831634 ; Phone: +55-91-31831740
E-mail: karlo@ufpa.br